ACS OMEGA

http://pubs.acs.org/journal/acsodf
Article

Fabrication of Zinc Doped Titanium Dioxide Nanoparticles to Inhibit *Escherichia coli* Growth and Proliferation of Liver Cancer Cells (HepG2)

Tariq Munir, Arslan Mahmood,* Numan Abbas, Amjad Sohail, Yasin Khan, Saba Rasheed, and Irfan Ali

Cite This: *ACS Omega* 2024, 9, 34841−34847

ABSTRACT: The current research is related to the synthesis of different concentrations (0, 3, and 7 wt %) Zn doped TiO_2-NPs by using the coprecipitation method. The rutile, anatase crystal structure appeared on different diffracted peaks in TiO_2-NPs, and the crystallite size (12 to 24 nm) was calculated by using XRD analysis. The spherical, irregular, porous grain-like surface morphology was observed by SEM analysis, and the identification of different functional modes such as hydroxyl, −C−O, −C−O−C, and Ti−O−Ti attached on the surface of the spectrum was examined via FTIR analysis. After that, the increased absorbance of TiO_2-NPs by increasing the Zn concentration in TiO_2-NPs was observed by UV−visible analysis. After that, the well diffusion method was performed to measure antibacterial activity, and the MTT assay was used to investigate anticancer activity against the HepG2 cell line. It was observed that the inhibition zone of *S. aureus* and *E. coli* increased by increasing the concentration of Zn-doped TiO_2-NPs from 2 to 32 mm. The 7 wt % Zn-doped TiO_2-NPs provided significant anticancer activity against the liver cancer cell line and antibacterial activity. In the future, Zn doped TiO_2-NPs can be used for in vitro analysis against different microbial and animal models for the treatment of cancer.

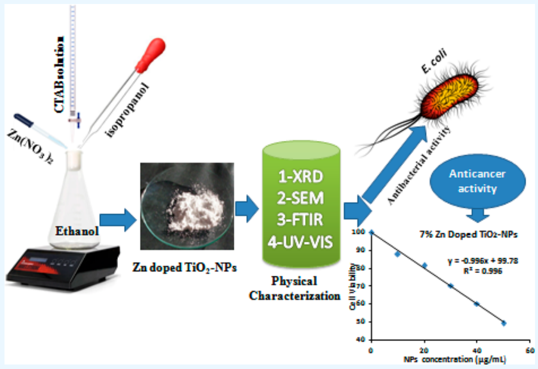

1. INTRODUCTION

The quantum size effect and optical performance of nanomaterials significantly contribute to biomedical applications.[1,2] The nanomaterials have a small size as compared to cellular organelles, and nanomaterials can easily penetrate inside the cells/tissues.[3,4] After penetration, the transition metal oxide nanoparticles into tissues have a greater ability to generate free radicals as compared to sulfide, carbide, or nitride-based nanomaterials. In addition, oxide base nanomaterials are preferred for biomedical applications, because these nanomaterials have a greater ability to generate free radicals and also have a significant ability to damage proteins, lipids, and nucleic acid.[5] According to previous reports, the various types of nanoparticles such as Fe_3O_4, NiO, Mn_3O_4, CuO, V_3O_5, ZnO, TiO_2, SnO_2, and Co_3O_4 are used for antiviral, antifungal, antibacterial, and anticancer agents, respectively.[6−9] Likewise, these nanomaterials are suitable for diverse therapies such as hyperthermia, MRI contrast agents, magnetic therapy, radiation therapy, and chemotherapy, and also these materials are effective for electrochemical effects.[10−12]

According to a previous study, the surface functionalization and doping agents in oxide, sulfide, and nitride based nanomaterials enhance the structural, electrical, optical, and biological performance.[13−15] The TiO_2 nanoparticles exist in three different structural phases which include rutile, brookite, and anatase.[16] The rutile and anatase phases are the most common compared to brookite. TiO_2-NPs are chemically stable, nontoxic, and low cost, which is why they are promising for antibacterial and anticancer activities. The biomedical application was improved to reduce the surface area and functionalized or doped the metal oxide NPs with other organic and inorganic elements.[17−19]

In addition, doping of cations also enhances the potential for biomedical application. The metal ions are incorporated in the crystal structure at the titanium sites in this case. Cations of transition metals (Zn^{2+}, W^{6+}, In^{3+}, La^{3+}, and Nb^{5+}) and rare earth metals might be employed for these alterations.[20−22] Indumathi et al. (2023) reported that the Cu doping of NiO NPs improved their antibacterial and anticancer activities, and Paul et al. (2023) also provided information about NiO nanoparticles significantly improving the biomedical applica-

Received: May 7, 2024
Revised: July 18, 2024
Accepted: July 19, 2024
Published: July 29, 2024

https://doi.org/10.1021/acsomega.4c04183
ACS Omega 2024, 9, 34841−34847

tions.[23,24] Paul et al. (2013) examined whether due to thermal stability the CuO NPs could be used as fuel cells, and Kalaivani et al. (2024) provided a study using TiO_2-NPs as an ethanol sensor due to their tuneable properties.[25,26] In addition, the magnetic nanoparticles played a central role for the remote control process to treat internal organs.[27,28] In early decades zinc ion doped TiO_2 nanoparticles were used for the enhancement of photocatalytic performance, and the insertion of aluminum ions resulted in a reduction. The zinc-doped anatase TiO_2 nanowires were discovered to have outstanding photocatalytic efficiency and a greater rate of kinetic reaction.[29−31] Another co-doping approach increases the concentration of structural defects in TiO_2-NPs. In particular, the combined insertion of Fe^{3+} and Zn^{2+} ions as modifying agents increased the photocatalytic activity relative to the materials doped only with Fe or Zn ions. Materials doped with Ag and Fe ions are another type of cationic co-doping.[32] Co-doping was demonstrated to enhance the specific surface area, increase the life span of photogenerated charge carriers, and improve visible light absorption and biomedical activities.[33,34] The different metal doped TiO_2-NPs played a central role for multiple applications as well as biomedical application. But in the current analysis, the liver cancer cell line activity was examined for the first time by Zn doped TiO_2-NPs.

The present study is related to the synthesis of Zn-doped TiO_2-NPs by using the coprecipitation method. Physical characterization such as XRD, SEM, FTIR, and UV−vis was used to investigate the structural, surface morphology, rotational, and vibrational modes properties and optical behavior of Zn-doped TiO_2-NPs. After that, an in vitro bioassay was used to calculate the antibacterial and anticancer activities via the well diffusion method and MTT assay.

2. EXPERIMENTAL SECTION

2.1. Chemicals. Following are the chemicals used for the synthesis of TiO_2-NPs: titanium(IV) butoxide (98%), ethyl alcohol (99%), hexadecyltrimethylammonium bromide (99%), and zinc nitrate (98%) were purchased from Sigma-Aldrich in the United States. In addition, the filter paper and deionized water were purchased from the local market in Faisalabad, Pakistan.

2.2. Preparation of TiO_2 Nanoparticles. Titanium(IV) butoxide $Ti(OCH_2CH_2CH_2CH_3)_4$ (0.1 M) was dissolved in 300 mL of ethanol, and 37 mL of isopropanol was placed on the magnetic stirrer with continuous stirring for 4 h at 80 °C. During stirring, the aqueous solution of CTAB (2 g in 100 mL of deionized water) was added dropwise. After 4 h of stirring the solution was cooled at room temperature for a day. The white precipitates were obtained at the bottom. Then the solution was filtered and washed with ethanol two to three times to remove the impurities from the solution. After filtration and washing with ethanol, a precipitate was obtained. The precipitate was dried at 110 °C for 12 h. The dried precipitate was homogenized in with a mortar and pestle. Finally, the collected powder was calcinated at 500 °C for 4 h.

2.3. Zinc-Doped TiO_2 Nanoparticles. The previously discussed procedure was repeated for the synthesis of the TiO_2 material. The 3 wt % of zinc nitrate was added to the TiO_2 solution and stirred for 30 min. After that, the prepared solution was filtered three times with ethanol to get a Zn-doped TiO_2 material. The same process was repeated for 7 wt % Zn-doped TiO_2-NPs. The calcination of all samples was completed at 500 °C for 4 h in a muffle furnace.

2.4. Physical Material Characterization Techniques. The X-ray advance diffractometer was used to identify the crystal structure and phase purity. Tabletop SEM (Emcrafts Cube 2020) was used to investigate the morphology and grain size. The Bruker Alpha FTIR spectrophotometer examined the functional groups attached to the spectrum. After that, the spectrophotometer (Model # UH5300 Spectrophotometer) was used to observe the optical behavior of Zn-doped TiO_2 nanoparticles.

2.5. Antibacterial Assay. Munir et al. (2022) reported the bacteria culture process. The antibacterial activity was examined against Gram-negative bacteria by using pure and Zn-doped TiO_2-NPs. The activity was investigated via 40 mg/mL pure and Zn-doped TiO_2-NPs. The inhibition zone was calculated by using eq 1 after 24 h at 37 °C.[35]

$$\%\ activity = \frac{Zone\ of\ inhibition\ of\ test\ compound}{Zone\ of\ inhibition\ of\ standard} \times 100\% \tag{1}$$

2.6. HepG2 Cell Culturing, Labeling, and MTT Assay. The liver carcinoma cell line was cultured by using 96 well plates and a tissue culture flask (25 cm) which contributes Hank salts 10% fetal bovine serum in DMEM. After that, the nonessential amino acids and glutamine 2 mM/L are incubated for 24 h at 37 °C. The various concentrations (0 to 50 mg/mL) of pure and Zn-doped TiO_2-NPs solution were incorporated in cultured cells. The percentage cell viability was calculated by using the mathematical expression.

$$\%\ cell\ viability = \frac{Average\ optical\ density\ of\ tested\ sample}{Average\ optical\ density\ of\ control} \times 100\% \tag{2}$$

2.7. Statistical Analysis. The relation between the control and different concentrations of Zn-doped TiO_2-NPs was investigated by using regression analysis. In the case of regression analysis, the value R^2 provided the most significant value.

3. RESULTS AND DISCUSSION

3.1. XRD Analysis. Figure 1 shows the XRD spectra of pure and Zn-doped TiO_2-NPs. The different diffracted peaks representing the rutile and anatase crystal structures at 25.33°, 27.41°, 36.03°, 37.78°, 38.65°, 48.04°, 53.93°, and 55.24° indicate the various Miller indices such as (A101), (R101), (103), (004), (112), (200), (105), and (211).[36] The rutile peak (R101) appeared after adding the doping agent Zn in TiO_2-NPs with high concentrations.[37] Furthermore, the ZnO peak was obtained at 41.27° due to the high concentration of Zn (7%). The crystallite size of peak (A101) was calculated by using the Scherrer equation (eq 3) in the range 24 to 12 nm expressed in Table 1. It shows that the crystallite size was decreased by varying the Zn concentration in TiO_2 nanoparticles.[38] The grain boundary pinning was the major factor in the reduction of size, and it also confined the growth factor of grain.

$$D = \frac{k\lambda}{\beta\cos\theta} \tag{3}$$

3.2. SEM Analysis. To identify the surface morphology of pure and different concentrations of Zn-doped TiO_2-NPs, they were examined by SEM analysis. The results are shown in

https://doi.org/10.1021/acsomega.4c04183
ACS Omega 2024, 9, 34841−34847

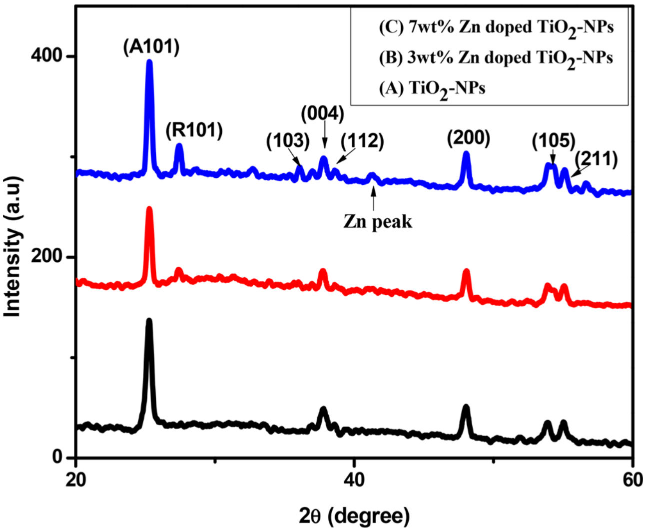

Figure 1. XRD spectrum of Zn doped TiO_2-NPs.

Table 1. Structural Parameters of Zn Doped TiO_2-NPs

Samples	FWHM	Crystallite Size (101) (nm)
TiO_2-NPs	0.301	24
3 wt % Zn doped TiO_2-NPs	0.525	14
7 wt % Zn doped TiO_2-NPs	0.631	12

Figure 2A for TiO_2-NPs, Figure 2B for 3 wt % Zn doped TiO_2-NPs, and Figure 2C for 7 wt % Zn doped TiO_2-NPs. The

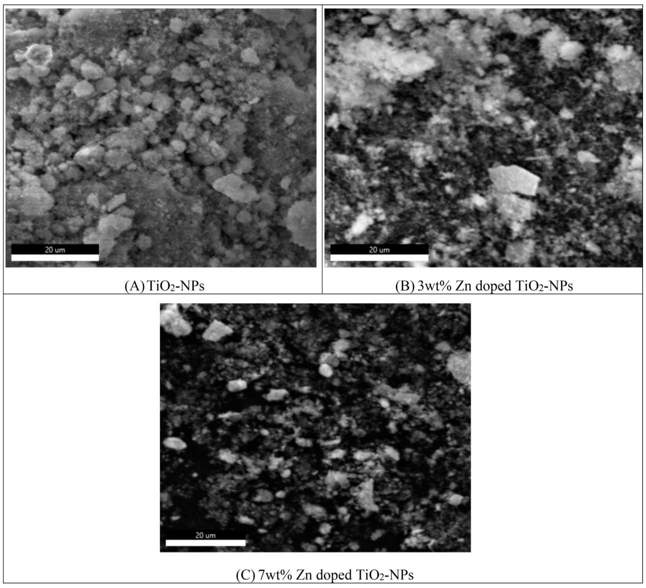

Figure 2. Surface morphology of (A) TiO_2-NPs, (B) 3 wt % Zn doped TiO_2-NPs, and (C) 5 wt % Zn doped TiO_2-NPs.

following micrographs depicted spherical, irregular, nonuniform, and porous-like surfaces.[39] These graphs indicated that increasing the wt % ratio of Zn doped TiO_2-NPs increased the grain size, and it was also observed that the agglomeration increased with Zn concentration in TiO_2-NPs.[40] It was also observed that the pH of the solution decreased due to the increased concentration of Zn which causes large aggregation. The low-temperature synthesis process also causes aggregation in pure and Zn-doped TiO_2-NPs. The overall SEM analysis shows that the aggregation in pure and Zn-doped TiO_2-NPs is due to the effect of the pH and low-temperature synthesis technique.[41]

3.3. FTIR Analysis. The FTIR spectrum ranged from 4000 to 500 cm^{-1} for pure and Zn-doped TiO_2-NPs (Figure 3). All

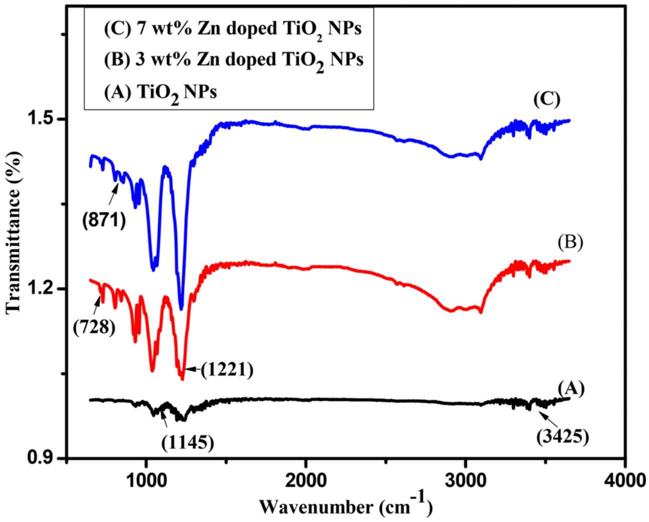

Figure 3. FTIR spectra of TiO_2-NPs and Zn doped TiO_2-NPs.

absorbance bands appeared between 720 to 830 cm^{-1} which indicates the presence of Ti−O−Ti in the lattice of TiO_2-NPs. In the case of Zn use as a doping agent in TiO_2-NPs, bands were observed in the B and C spectra at 871 cm^{-1} and show more absorbance with increasing Zn concentration in the samples.[41] After that, absorbance of water molecules in Zn-doped TiO_2-NPs, which express vibrational stretching modes (hydroxyl group), was observed at 3681 cm^{-1} and 1145 cm^{-1}.[42] The stronger vibrational mode shows a greater interaction between the water and TiO_2-NPs. In addition, a few bands were observed at 1093 cm^{-1} to 1397 cm^{-1} which indicate the presence of the −C−O band and −C−O−C modes and the presence of these modes in the sample through the atmosphere during the synthesis process. The one extra peak was observed by doping Zn metal in TiO_2-NPs, and this shows excellent agreement with XRD analysis.

3.4. Optical Behavior of Zn-Doped TiO_2-NPs. UV−visible spectroscopy was used to investigate the optical behavior of pure and Zn-doped TiO_2-NPs, as shown in Figure 4A for TiO_2-NPs, Figure 4B for 3 wt % Zn doped TiO_2-NPs, and Figure 4C for 7 wt % Zn doped TiO_2-NPs. The absorbance band of TiO_2-NPs was observed at 375 nm, and it was also observed that the absorbance increases and wavenumber shifts toward shorter by increasing the Zn metal content in TiO_2-NPs.[43] Only a small band has appeared at 375 in the case of TiO_2-NPs, and a stronger absorbance band was observed of Zn-doped TiO_2-NPs in the ultraviolet region. There was a small effect on wavenumber by increasing the zinc concentration in TiO_2-NPs. This means that slight variations in band gap by metal doped in TiO_2-NPs were reported in previous literature.[44] Ahamed et al. (2016) reported that the band gap increased from 3.35 to 3.85 eV by increasing the Zn concentration in TiO_2-NPs up to 10 wt %.[45]

3.5. Antibacterial Activity. The antibacterial activities of TiO_2-NPs and 3 and 7 wt % Zn doped TiO_2-NPs are examined against Gram-positive (*S. aureus*) Gram-negative (*E. coli*)

https://doi.org/10.1021/acsomega.4c04183
ACS Omega 2024, 9, 34841−34847

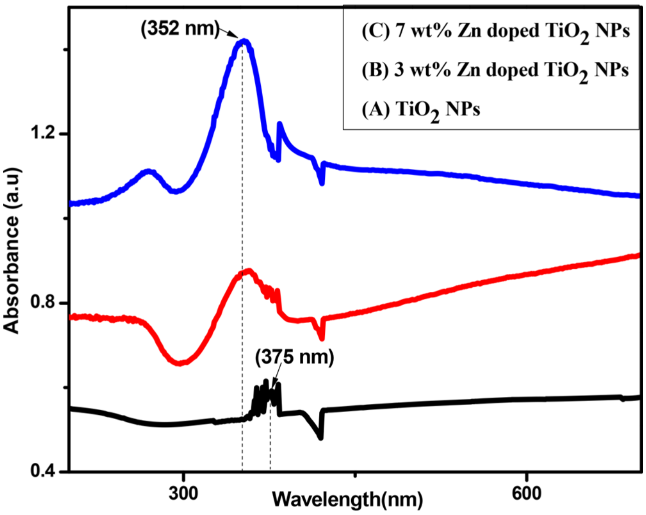

Figure 4. UV−vis analysis of Zn-doped TiO_2-NPs.

bacteria. The activity was observed in the entire sample at the same concentration, such as 40 mg/mL. The inhibition zone increased with high concentration Zn-doped TiO_2 nanoparticles (Figure 5). The inhibition zone was calculated for TiO_2-NPs (1 mm), 3 wt % Zn doped TiO_2-NPs (15 mm), and 7 wt % TiO_2-NPs (20 mm) against *S. aureus*, and the inhibition zone against *E. coli* was observed for TiO_2-NPs (28 mm), 3 wt % Zn doped TiO_2-NPs (30 mm), and 7 wt % TiO_2-NPs (32 mm). The well diffusion method indicated that 7 wt % Zn doped TiO_2-NPs are most suitable for anti *S. aureus* and *E. coli* activities. The ions generated by pure and Zn-doped TiO_2-NPs can penetrate the cell wall of given bacteria which causes damage to the cell wall and bacterial death.[46] The disc present in Figure 5 shows that due to increased concentration of Zn doped TiO_2-NPs antibacterial activity increased.

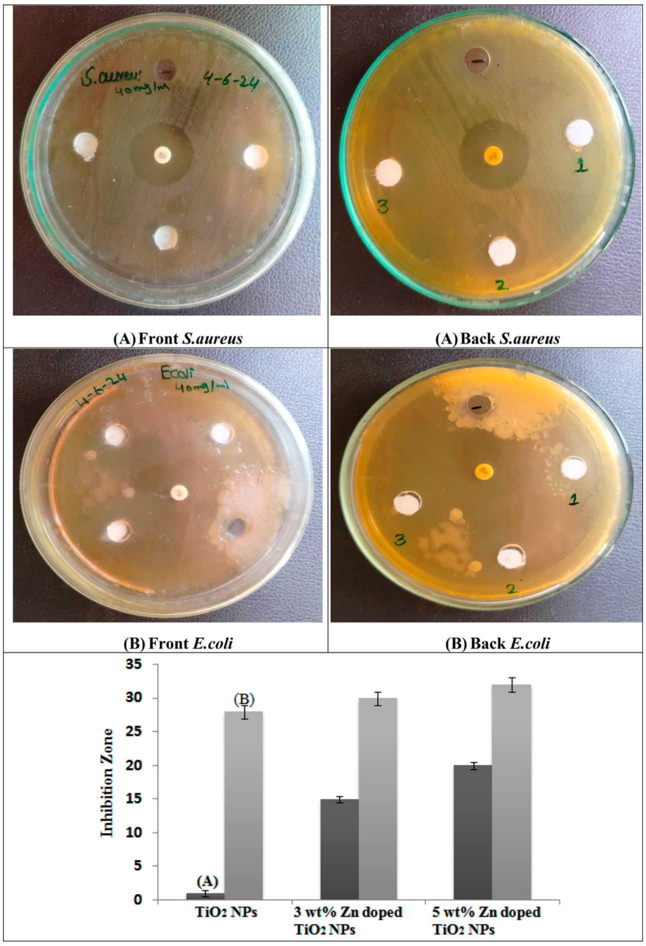

Figure 5. Antibacterial activity of Zn doped TiO_2-NPs.

3.6. Cell Viability. The different concentrations of Zn-doped TiO_2-NPs (0 to 50 μg/mL) were used to treat the liver cancer cell line by using an MTT assay. The cell viability of pure and Zn-doped TiO_2-NPs was tested (Figure 6). The MTT assay was used to evaluate the mitochondria function, and cell viability of the HepG2 cell line is dose-dependent due to an increase in the concentration of Zn doped TiO_2-NPs and then a cell viability decrease.[47] In addition, TiO_2-NPs did not provide significant results against HepG2 cells, and due to the increase in the concentration of Zn in TiO_2-NPs the cell viability improved up to a significant level. However, the most significant results were observed by using 7 wt % Zn-doped TiO_2-NPs. In addition, another way for the treatment of cancer is in which reactive oxygen species also cause cancer cell death.[48,49] Finally, regression analysis was preferred to observe the most significant value, and 7 wt % Zn doped TiO_2-NPs show a significant value (R^2 = 0.996). Figure 7 shows the statistical analysis of Zn-doped TiO_2-NPs against the HepG2 cell line.

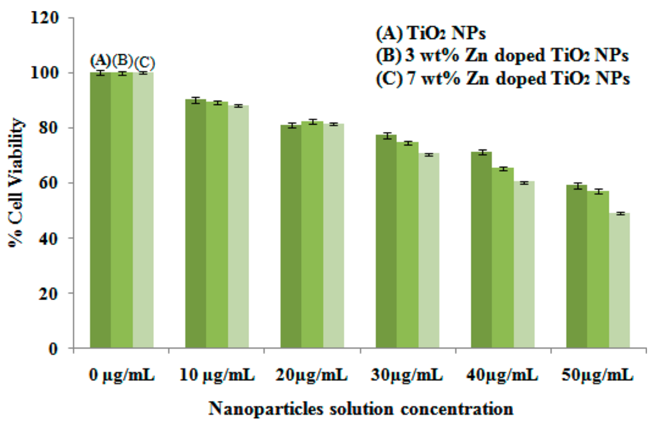

Figure 6. Cell viability of Zn doped TiO_2-NPs.

4. CONCLUSION

The pure and different concentrations of Zn (3 and 7 wt %) doped TiO_2-NPs were synthesized via the coprecipitation method. The physical properties, which include rutile and anatase crystal structures, were investigated by XRD analysis. The spherical, irregular, and nonuniform surface morphology was observed via SEM analysis, and different functional groups attached to the spectrum of pure and Zn-doped TiO_2-NPs were observed by using FTIR analysis. The UV−vis analysis was used to examine the absorbance of Zn-doped TiO_2-NPs. After that, an in vitro bioassay was significantly tested against *E. coli* by using 40 mg/mL of Zn doped TiO_2-NPs and 7 wt % of Zn doped TiO_2-NPs provided excellent anticancer activity against the (HepG2) liver cancer cell line. The overall analyses revealed that Zn-doped TiO_2-NPs provided significant results against the *E. coli* and HepG2 cell lines. In the future, Zn-

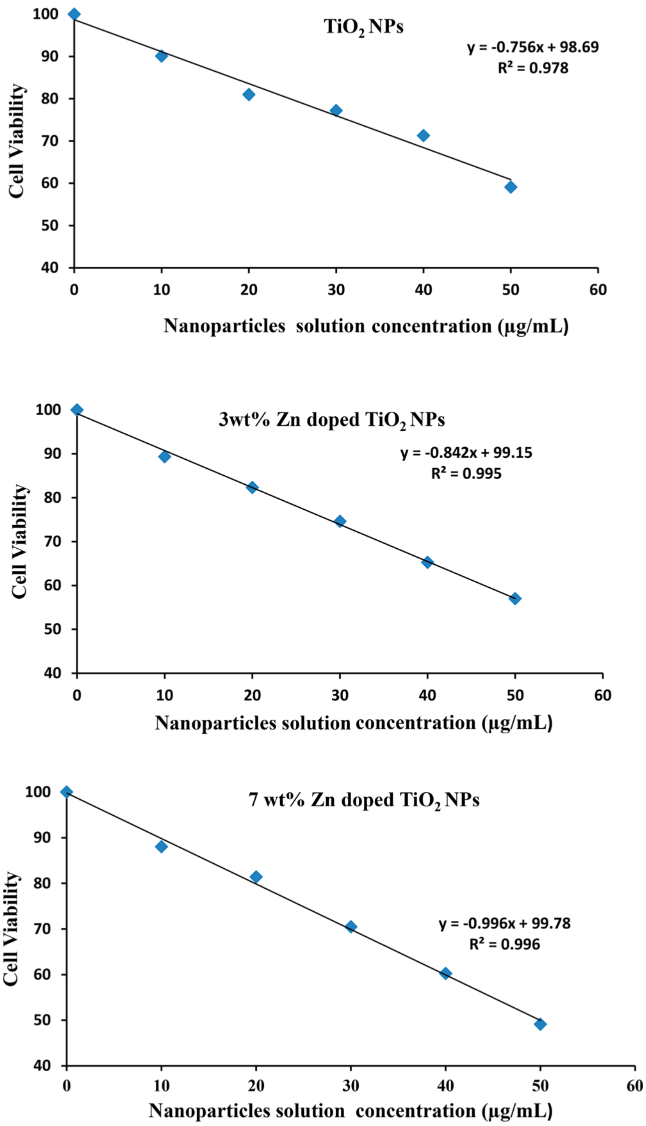

Figure 7. Statistical analysis of the HepG2 cell line of Zn doped TiO_2-NPs.

doped TiO_2-NPs can be used for hyperthermia and photodynamic therapy.

AUTHOR INFORMATION

Corresponding Author

Arslan Mahmood − *Department of Physics, Government College University Faisalabad (GCUF), Faisalabad 38000, Pakistan*; orcid.org/0009-0004-5029-7348; Email: arslan4physics@gmail.com

Authors

Tariq Munir − *Department of Physics, Government College University Faisalabad (GCUF), Faisalabad 38000, Pakistan*

Numan Abbas − *College of Physics and Information Technology, Shaanxi Normal University, Xian 710119 Shaanxi, PR China*

Amjad Sohail − *Department of Physics, Government College University Faisalabad (GCUF), Faisalabad 38000, Pakistan*

Yasin Khan − *Department of Electrical Engineering, College of Engineering, King Saud University, Riyadh 11362, Saudi Arabia*

Saba Rasheed − *Department of Physics, Government College University Faisalabad (GCUF), Faisalabad 38000, Pakistan*

Irfan Ali − *Department of Physics, Government College University Faisalabad (GCUF), Faisalabad 38000, Pakistan*

Complete contact information is available at:
https://pubs.acs.org/10.1021/acsomega.4c04183

Notes

The authors declare no competing financial interest.

ACKNOWLEDGMENTS

This work was supported by the Researchers Supporting Project number (RSPD2024R985), King Saud University, Riyadh, Saudi Arabia.

REFERENCES

(1) Tamgadge, Y. S.; Muley, G. G.; Deshmukh, K. U.; Pahurkar, V. G. Synthesis and nonlinear optical properties of Zn doped TiO_2 nanocolloids. *Opt. Mater.* **2018**, *86*, 185−190.

(2) Munir, T.; Mahmood, A.; Fakhar-e-Alam, M.; Imran, M.; Sohail, A.; Amin, N.; Mahmood, K.; et al. Treatment of breast cancer with capped magnetic-NPs induced hyperthermia therapy. *J. Mol. Struct.* **2019**, *1196*, 88−95.

(3) Sokolova, V.; Epple, M. Inorganic nanoparticles as carriers of nucleic acids into cells. *Angewandtechemie international edition* **2008**, *47* (8), 1382−1395.

(4) Mahmood, A.; Munir, T.; Rasul, A.; Ghfar, A. A.; Mumtaz, S. Polyethylene glycol and Chitosan Functionalized Manganese Oxide Nanoparticles for Antimicrobial and Anticancer Activities. *J. Colloid Interface Sci.* **2023**, *648*, 907.

(5) Eftekhari, A.; Ahmadian, E.; Panahi-Azar, V.; Hosseini, H.; Tabibiazar, M.; Maleki Dizaj, S. Hepatoprotective and free radical scavenging actions of quercetin nanoparticles on aflatoxin B1-induced liver damage: in vitro/in vivo studies. *Artificial cells, nanomedicine, and biotechnology* **2018**, *46* (2), 411−420.

(6) Munir, T.; Mahmood, A.; Rasul, A.; Imran, M.; Fakhar-e-Alam, M. Biocompatible polymer functionalized magnetic nanoparticles for antimicrobial and anticancer activities. *Mater. Chem. Phys.* **2023**, *301*, 127677.

(7) Indumathi, T.; Theivarasu, C.; Pradeep, I.; Rani, M. T.; Magesh, G.; Rahale, C. S.; Kumar, E. R. Effects of Nd doping on structural, optical, morphological and surface-chemical state analysis of ZnO nanoparticles for antimicrobial and anticancer activities. *Surfaces and Interfaces* **2021**, *23*, 101000.

(8) Elamin, N. Y.; Indumathi, T.; Ranjith Kumar, E. Evaluation of physicochemical and biological properties of SnO2 and Fe doped SnO2 nanoparticles. *Ceram. Int.* **2023**, *49* (2), 2388−2393.

(9) Sudha, D.; Kumar, E. R.; Shanjitha, S.; Munshi, A. M.; Al-Hazmi, G. A.; El-Metwaly, N. M.; Kirubavathy, S. J. Structural, optical, morphological and electrochemical properties of ZnO and graphene oxide blended ZnO nanocomposites. *Ceram. Int.* **2023**, *49* (5), 7284−7288.

(10) Fakhar-e-Alam, M.; Shafiq, Z.; Mahmood, A.; Atif, M.; Anwar, H.; Hanif, A.; Ahmed, H.; et al. Assessment of green and chemically synthesized copper oxide nanoparticles against hepatocellular carcinoma. *Journal of King Saud University-Science* **2021**, *33* (8), 101669.

(11) Avasthi, A.; Caro, C.; Pozo-Torres, E.; Leal, M. P.; García-Martín, M. L. Magnetic nanoparticles as MRI contrast agents. *Surface-modified Nanobiomaterials for Electrochemical and Biomedicine Applications* **2020**, 49−91.

(12) Kadhim, W. K. A.; Nayef, U. M.; Jabir, M. S. Polyethylene glycol-functionalized magnetic (Fe_3O_4) nanoparticles: a good method for a successful antibacterial therapeutic agent via damage DNA molecule. *Surf. Rev. Lett.* **2019**, *26* (10), 1950079.

(13) Radhi, M. M.; Abdullah, H. N.; Jabir, M. S.; Al-Mulla, E. A. J. Electrochemical effect of ascorbic acid on redox current peaks of

$CoCl_2$ in blood medium. *Nano Biomedicine and Engineering* **2017**, *9* (2), 103−106.

(14) Khashan, K. S.; Jabir, M. S.; Abdulameer, F. A. Preparation and characterization of copper oxide nanoparticles decorated carbon nanoparticles using laser ablation in liquid. *Journal of Physics: Conference Series* **2018**, *1003*, 012100.

(15) Munir, T.; Mahmood, A.; Shafiq, F.; Fakhar-e-Alam, M.; Atif, M.; Raza, A.; Abbas, N.; et al. Experimental and theoretical analyses of nano-silver for antibacterial activity based on differential crystal growth temperatures. *Saudi Journal of Biological Sciences* **2021**, *28* (12), 7561−7566.

(16) Yahaya, M. Z.; Azam, M. A.; Teridi, M. A. M.; Singh, P. K.; Mohamad, A. A.; et al. Recent characterisation of sol-gel synthesised TiO_2 nanoparticles. *Recent applications in Sol-Gel synthesis* **2017**, 109−129.

(17) Jang, W. S.; Pham, V. N.; Yang, S. H.; Baik, J.; Lee, H.; Kim, Y. M. Enhanced selective photocatalytic oxidation of a bio-derived platform chemical with vacancy-induced core-shell anatase TiO_2 nanoparticles. *Applied Catalysis B: Environmental* **2023**, *322*, 122140.

(18) Lu, C. M.; Sharma, R. K.; Wang, C. W.; Chatterjee, N.; Lee, W. C.; Chen, C. Y. Biogenic synthesis of nano-photocatalysts doped TiO_2 nanoparticles and their application in photocatalytic degradation. *J. Mol. Struct.* **2023**, *1271*, 134023.

(19) Sukhadeve, G. K.; Bandewar, H.; Janbandhu, S. Y.; Jayaramaiah, J. R.; Gedam, R. S. Photocatalytic hydrogen production, dye degradation, and antimicrobial activity by Ag-Fe co-doped TiO_2 nanoparticles. *J. Mol. Liq.* **2023**, *369*, 120948.

(20) P, A.; T, K.; S, D.; J, J.; Abd El-Rehim, A.F.; Kumar, E. R. Evaluation of structural, optical and morphological properties of La doped TiO_2 nanoparticles. *Ceram. Int.* **2023**, *49* (11), 16991−16998.

(21) Elamin, N. Y.; Indumathi, T.; Ranjith Kumar, E. Pluronic f127 encapsulated titanium dioxide nanoparticles: evaluation of physiochemical properties for biological applications. *J. Mol. Liq.* **2023**, *379*, 121655.

(22) Ananthi, S.; Kavitha, M.; Balamurugan, A.; Ranjith Kumar, E.; Magesh, G.; Abd El-Rehim, A. F.; Rahale, C. S.; et al. Synthesis, analysis and characterization of camellia sinensis mediated synthesis of NiO nanoparticles for ethanol gas sensor applications. *Sens. Actuators, B* **2023**, *387*, 133742.

(23) Indumathi, T.; Hirad, A. H.; Alarfaj, A. A.; Ranjith Kumar, E.; Chandrasekaran, K. Phytoextract-mediated synthesis of Cu doped NiO nanoparticle using cullon tomentosum plant extract with efficient antibacterial and anticancer property. *Ceram. Int.* **2023**, *49* (19), 31829−31838.

(24) Paul, C. A.; Kumar, E. R.; Suryakanth, J.; Abd El-Rehim, A. F. Structural, microstructural, vibrational, and thermal investigations of NiO nanoparticles for biomedical applications. *Ceram. Int.* **2023**, *49* (16), 27230−27246.

(25) Paul, C. A.; Ranjith Kumar, E. R.; Suryakanth, J.; Abd El-Rehim, A. F. Analysis and characterization of structural, morphological, thermal properties and colloidal stability of CuO nanoparticles for various natural fuels. *Ceram. Int.* **2023**, *49* (19), 31193−31209.

(26) Kalaivani, T.; Anilkumar, P.; Jasmin, J.; Deepak, S.; Ranjith Kumar, E. R. A study on microstructural, optical, vibrational, and morphological features of TiO2 nanoparticles for ethanol sensor application. *Inorg. Chem. Commun.* **2024**, *161*, 112061.

(27) Susithra, V.; Kavi, S. S.; Abd El-Rehim, A. F.; Kumar, E. R. Citrus sinensis assisted biogenic synthesis and physicochemical properties of Fe3O4 nanoparticles for antibacterial activity. *Ceram. Int.* **2024**, *50* (7), 10225−10231.

(28) Munir, T.; Imran, M.; Muzammil, S.; Hussain, A. A.; Alam, M. F. E.; Mahmood, A.; Afzal, M.; et al. Antimicrobial activities of polyethylene glycol and citric acid coated graphene oxide-NPs synthesized via Hummer's method. *Arabian Journal of Chemistry* **2022**, *15* (9), 104075.

(29) Chauhan, R.; Kumar, A.; Chaudhary, R. P. Structural and optical characterization of Zn doped TiO_2 nanoparticles prepared by sol−gel method. *J. Sol-Gel Sci. Technol.* **2012**, *61* (3), 585−591.

(30) Jabir, M. S.; Taha, A. A.; Sahib, U. I. Linalool loaded on glutathione-modified gold nanoparticles: a drug delivery system for a successful antimicrobial therapy. *Artificial cells, nanomedicine, and biotechnology* **2018**, *46* (sup2), 345−355.

(31) Al-Ziaydi, A. G.; Al-Shammari, A. M.; Hamzah, M. I.; Kadhim, H. S.; Jabir, M. S. Hexokinase inhibition using D-Mannoheptulose enhances oncolytic newcastle disease virus-mediated killing of breast cancer cells. *Cancer Cell International* **2020**, *20*, 420.

(32) Sanchez-Dominguez, M.; Morales-Mendoza, G.; Rodriguez-Vargas, M. J.; Ibarra-Malo, C. C.; Rodriguez-Rodriguez, A. A.; Vela-Gonzalez, A. V.; Gomez, R.; et al. Synthesis of Zn-doped TiO2 nanoparticles by the novel oil-in-water (O/W) microemulsion method and their use for the photocatalytic degradation of phenol. *Journal of Environmental Chemical Engineering* **2015**, *3* (4), 3037−3047.

(33) Santhi, K.; Ponnusamy, S.; Harish, S.; Navaneethan, M. A facile synthesis of Zn-doped TiO_2 nanostructures for enhanced photocatalytic performance. *Journal of Materials Science: Materials in Electronics* **2022**, *33* (12), 9798−9813.

(34) Elmehasseb, I.; Kandil, S.; Elgendy, K. Advanced visible-light applications utilizing modified Zn-doped TiO_2 nanoparticles via non-metal in situ dual doping for wastewater detoxification. *Optik* **2020**, *213*, 164654.

(35) Meesombad, K.; Sato, N.; Pitiphattharabun, S.; Panomsuwan, G.; Techapiesancharoenkij, R.; Surawathanawises, K.; Jongprateep, O.; et al. Zn-doped TiO_2 nanoparticles for glutamate sensors. *Ceram. Int.* **2021**, *47* (15), 21099−21107.

(36) Munir, T.; Mahmood, A.; Peter, N.; Rafaqat, N.; Imran, M.; Ali, H. E. Structural, morphological and optical properties at various concentration of Ag doped SiO2-NPs via sol gel method for antibacterial and anticancer activities. *Surfaces and Interfaces* **2023**, *38*, 102759.

(37) Nguyen, T. B.; Hwang, M. J.; Ryu, K. S. Synthesis and high photocatalytic activity of Zn-doped TiO2 nanoparticles by sol-gel and ammonia-evaporation method. *Bulletin of the Korean Chemical Society* **2012**, *33* (1), 243−247.

(38) Varadharajan, K.; Singaram, B.; Mani, R.; Jeyaram, J. Enhanced visible light photocatalytic activity of Ag and Zn doped and codopedTiO 2 nanoparticles. *Journal of Cluster Science* **2016**, *27*, 1815−1829.

(39) Santhi, K.; Ponnusamy, S.; Harish, S.; Navaneethan, M. A facile synthesis of Zn-doped TiO2 nanostructures for enhanced photocatalytic performance. *Journal of Materials Science: Materials in Electronics* **2022**, *33* (12), 9798−9813.

(40) Regraguy, B.; Ellouzi, I.; Mabrouki, J.; Rahmani, M.; Drhimer, F.; Mahmou, C.; El Hajjaji, S.; et al. Zinc doping of different nanoparticles of TiO_2 Sachtopore for improved elimination of the methyl orange by photocatalysis. *Emergent Materials* **2022**, *5* (6), 1945−1958.

(41) Munir, T.; Sharif, M.; Ali, H.; Kashif, M.; Sohail, A.; Sabir, N.; Ahmed, N. Impact of silver dopant on structural and optical properties of TiO_2 nanoparticles. *Dig. J. Nanomater. Biostructures* **2019**, *14*, 279−284.

(42) Wang, Y.; Wang, X.; Li, L.; Wu, Y.; Yu, Q. An experimental and theoretical study on the photocatalytic antibacterial activity of boron-doped TiO_2 nanoparticles. *Ceram. Int.* **2022**, *48* (1), 604−614.

(43) Karthikeyan, K.; Chandraprabha, M. N.; Krishna, R. H.; Samrat, K.; Sakunthala, A.; Sasikumar, M. Optical and antibacterial activity of biogenic core-shell ZnO@ TiO_2 nanoparticles. *Journal of the Indian Chemical Society* **2022**, *99* (3), 100361.

(44) Santhi, K.; Ponnusamy, S.; Harish, S.; Navaneethan, M. A facile synthesis of Zn-doped TiO2 nanostructures for enhanced photocatalytic performance. *Journal of Materials Science: Materials in Electronics* **2022**, *33* (12), 9798−9813.

(45) Ahamed, M.; Khan, M. M.; Akhtar, M. J.; Alhadlaq, H. A.; Alshamsan, A. Ag-doping regulates the cytotoxicity of TiO_2 nanoparticles via oxidative stress in human cancer cells. *Sci. Rep.* **2017**, *7* (1), 17662.

(46) Ahamed, M.; Khan, M. M.; Akhtar, M. J.; Alhadlaq, H. A.; Alshamsan, A. Role of Zn doping in oxidative stress mediated cytotoxicity of TiO_2 nanoparticles in human breast cancer MCF-7 cells. *Sci. Rep.* **2016**, *6* (1), 30196.

(47) Bai, Q.; Zhang, Y.; Cai, R.; Wu, H.; Fu, H.; Zhou, X.; Liu, T.; et al. AMP-Coated TiO2 Doped ZnO Nanomaterials Enhanced Antimicrobial Activity and Efficacy in Otitis Media Treatment by Elevating Hydroxyl Radical Levels. *Int. J. Nanomed.* **2024**, *19*, 2995–3007.

(48) Manikandan, T.; Padmalaya, G.; Murugeswari, S.; Ramakrishnan, M.; Krishnasamy, K.; Mallik, S.; Shah, M. A. Evaluation on Characteristics of Anticancer and Antimicrobial Activities with Cipla Loaded ZnO Nanostructural Rods for Human Breast Cancer Cell Line Targeting. *Research Square*, 2024.

(49) Mahmoudi, S.; Otadi, M.; Hekmati, M.; Monajjemi, M.; Shekarabi, A. S. Supported silver nanoparticles over Metronidazole modified-single walled carbon nanotubes for overcoming antimicrobial properties, anti-cancer effect, and apoptosis induction on human gastric cancer cell line. Results. *Chemistry* **2024**, *7*, 101519.

https://doi.org/10.1021/acsomega.4c04183
ACS Omega 2024, 9, 34841−34847